DALTON

Synthesis, redox behaviour and molecular structures of new metal cluster species containing orthometallated $[M_3(\mu\text{-}H)(CO)_{10}(\mu\text{-}NC_5H_4)]$ (M = Ru or Os) and ferrocene chromophores bridged by an aromatic unit

Wai-Yeung Wong and Wing-Tak Wong *

Department of Chemistry, The University of Hong Kong, Pokfulam Road, Hong Kong

The ferrocenyl-functionalized pyridyl $[Fe(\eta^5\text{-}C_5H_5)(\eta^5\text{-}C_5H_4C_6H_4C_5H_4N)]$ **1**, which contains an aromatic entity in the backbone, has been prepared and structurally characterized by X-ray diffraction. Ligation of this redox-active compound with trinuclear carbonyl clusters $[M_3(CO)_{10}L_2]$ (M = Ru, L = CO; M = Os, L = MeCN) by oxidative addition provided $[M_3(\mu\text{-}H)(CO)_{10}\{\mu\text{-}NC_5H_3C_6H_4(\eta^5\text{-}C_5H_4)Fe(\eta^5\text{-}C_5H_5)\}]$ (M = Ru **2** or Os **3**) in high yields. Characterization of **2** and **3** by IR and ^1H NMR spectroscopy revealed that these complexes have analogous orthometallated molecular geometries. To confirm this, crystal structure determinations were carried out for both **2** and **3**. Spectroscopic and structural evidence for both **2** and **3** suggests a new class of metal clusters consisting of an orthometallated trinuclear carbonyl cluster unit rigidly linked to a ferrocenyl moiety through an aromatic pathway. Electrochemical investigations revealed that both **2** and **3** undergo a reversible one-electron oxidation at iron followed by an irreverible oxidation of the metal cluster core.

The design of metallosupramolecular systems containing electronically coupled redox-active sites has been a subject of considerable interest due to the rapid growth of material science.[1] Metallocenes, and in particular ferrocene, have found applications in molecular ferromagnets,[2] molecular sensors,[3] electrochemical agents,[4] liquid crystals[5] and non-linear optics.[6] The importance of ferrocenyl derivatives in electroactive heteropolynuclear aggregates[7] and as donors in charge-transfer complexes[8] has also been revealed recently. On the other hand, transition-metal clusters have been shown to possess interesting magnetic[9] and redox properties.[10] So the idea of combining the properties of these two classes of compounds has significant appeal, especially at the supramolecular level.

However, although metallocenes are widely used as redox-active sites in supramolecular systems,[11] very few examples have been reported in which such redox-active centres are covalently coupled to transition-metal cluster frameworks in supramolecular arrays.[12] In order to get access to this class of compounds we have been developing strategies for the synthesis of redox-functionalized proligands for metallo-supramolecular chemistry. We chose ferrocenyl ligands because ferrocene-centred oxidations are known to display reversible, single-electron processes at modest anodic potentials.[13] The recent work by us on the metallosupramolecular cluster assemblies based on donor–acceptor bimetallic characteristics has opened new lines in the search for new topological molecular and supramolecular systems, where compounds incorporating pyridyl domains such as $[Fe(\eta^5\text{-}C_5H_5)(\eta^5\text{-}C_5H_4C_6H_4C_5H_4N)]$ **1** have proved to be versatile systems for such development.[12a] In this article we describe the preparation and spectroscopic studies of two new supramolecular cluster species $[M_3(\mu\text{-}H)(CO)_{10}\{\mu\text{-}NC_5H_3C_6H_4(\eta^5\text{-}C_5H_4)Fe(\eta^5\text{-}C_5H_5)\}]$ (M = Ru **2** or Os **3**), as 4-(*p*-ferrocenylphenyl)pyridine derivatives of the trinuclear carbonyl clusters $[M_3(CO)_{12}]$ (M = Ru or Os). The molecular structures of both supermolecules as well as that of the corresponding redox spectator **1** have been determined by single-crystal X-ray diffraction. The electrochemical behaviour of these complexes is also presented.

Experimental

All reactions and manipulations were carried out under Ar with the use of standard inert-atmosphere and Schlenk techniques. Solvents were dried by standard procedures and freshly distilled prior to use.[14] All chemicals, except where stated, were from commercial sources and used as received. The compounds $[Os_3(CO)_{10}(NCMe)_2]$[15] and 4-(*p*-ferrocenylphenyl)pyridine **1**[12a] were prepared by the literature methods. Proton NMR spectra were recorded on a JEOL GSX 270 Fourier-transform spectrometer using CD_2Cl_2 and referenced to $SiMe_4$ ($\delta = 0$), mass spectra on a Finnigan MAT 95 instrument by the fast-atom bombardment technique. Microanalyses were performed by Butterworth Laboratories, UK. Electronic absorption spectra were obtained with microprocessor-controlled Perkin-Elmer Lambda 3B UV-VIS spectrophotometer, thermostatted by a Lauda circulating bath. Cyclic voltammetric measurements were made with a Princeton Applied Research (PAR) model 273A potentiostat. The supporting electrolyte was 0.2 mol dm^{-3} $[NBu_4]BF_4$ in CH_2Cl_2. All experiments were carried out at ambient temperature and the system was calibrated using ferrocene as the internal standard. Routine separation of products in air was by thin-layer chromatography on plates coated with Merck Kieselgel 60 GF_{254}.

Preparations

$[Ru_3(\mu\text{-}H)(CO)_{10}\{\mu\text{-}NC_5H_3C_6H_4(\eta^5\text{-}C_5H_4)Fe(\eta^5\text{-}C_5H_5)\}]$ 2. A solution of $[Ru_3(CO)_{12}]$ (30 mg, 0.047 mmol) and $[Fe(\eta^5\text{-}C_5H_5)(\eta^5\text{-}C_5H_4C_6H_4C_5H_4N)]$ **1** (16 mg, 0.047 mmol) in tetrahydrofuran (thf) (15 cm^3) was refluxed under an argon atmosphere until all starting material had been consumed (3 h, TLC monitoring). The solvent was removed *in vacuo* and the residue chromatographed on silica with hexane–CH_2Cl_2 (4:1) as eluent. A major yellow band (R_f 0.6) proved to be compound **2** (26 mg, 60%). IR (hexane): $\tilde{\nu}_{CO}/cm^{-1}$ 2099m, 2061vs, 2050vs, 2024vs, 2014vs, 2009 (sh), 1998s and 1983w. ^1H NMR (CD_2Cl_2): δ 7.95 [dd, 1 H, $J(H_aH_b) = 6.1$, $J(H_aH_c) = 0.7$, H_a], 7.54 [dd, 1 H, $J(H_cH_a) = 0.7$, $J(H_cH_b) = 2.2$, H_c], 7.49 (s, 4 H, C_6H_4), 6.99 [dd, 1 H, $J(H_bH_a) = 6.1$, $J(H_bH_c) = 2.2$, H_b], 4.64 [t, 2 H, $J(H_\alpha H_\beta) = 1.9$, H_α], 4.30 [t, 2 H, $J(H_\beta H_\alpha) = 1.9$ Hz,

H_β], 3.97 (s, 5 H, C_5H_5) and −14.45 (s, 1 H, OsH). FAB-mass spectrum: *m/z* 924 (M^+) (Found: C, 40.0; H, 1.80; N, 1.45. Calc. for $C_{31}H_{17}FeNO_{10}Ru_3$: C, 40.35; H, 1.85; N, 1.50%).

[$Os_3(\mu\text{-}H)(CO)_{10}\{\mu\text{-}NC_5H_3C_6H_4(\eta^5\text{-}C_5H_4)Fe(\eta^5\text{-}C_5H_5)\}$] 3. A solution of [$Os_3(CO)_{10}(NCMe)_2$] (30 mg, 0.032 mmol) and compound **1** (11 mg, 0.032 mmol) in CH_2Cl_2 (10 cm^3) was heated to reflux for 3 h. The reaction mixture was then concentrated under vacuum and separated by TLC on silica using hexane–CH_2Cl_2 (7:3) as eluent. The major orange-yellow band, which contained compound **3**, was collected (R_f 0.8) and the solute isolated in 68% yield (26 mg). IR (hexane): $\tilde{\nu}_{CO}/cm^{-1}$ 2103m, 2063vs, 2053vs, 2022vs, 2010vs, 2003s, 1991vs and 1976m. ^1H NMR (CD_2Cl_2): δ 8.15 [dd, 1 H, $J(H_aH_b)$ = 6.1, $J(H_aH_c)$ = 0.7, H_a], 7.58 [dd, 1 H, $J(H_cH_a)$ = 0.7, $J(H_cH_b)$, = 2.2, H_c], 7.55 (s, 4 H, C_6H_4), 6.94 [dd, 1 H, $J(H_bH_a)$ = 6.1, $J(H_bH_c)$ = 2.2, H_b], 4.71 [t, 2 H, $J(H_\alpha H_\beta)$ = 1.9, H_α], 4.38 [t, 2 H, $J(H_\beta H_\alpha)$ = 1.9 Hz, H_β], 4.04 (s, 5 H, C_5H_5) and −14.78 (s, 1 H, OsH). FAB mass spectrum: *m/z* 1191 (M^+) (Found: C, 31.05; H, 1.35; N, 1.30. Calc. for $C_{31}H_{17}FeNO_{10}Os_3$: C, 31.3; H, 1.45; N, 1.20%).

Crystallography

Orange crystals of compound **1** were obtained by slow evaporation of a CH_2Cl_2 solution of **1** at room temperature for 3 d. Single crystals of **2** were grown by slow evaporation of a solution of it in hexane–CH_2Cl_2 at −10 °C for 2 d and those of **3** by crystallization from a CH_2Cl_2–MeOH solution of it at room temperature after 2 d. Diffraction data were collected at room temperature on a Rigaku AFC7R diffractometer using graphite-monochromated Mo-Kα radiation (λ = 0.710 73 Å) and a ω–2θ scan technique. The crystallographic and structure refinement data are summarized in Table 3. Lorentz-polarization and ψ-scan absorption corrections were applied to all the intensity data.[16] Neutral atom scattering factors were from ref. 17(*a*) and anomalous dispersion effects[17b] were included in F_c.

The space group of each crystal was determined from the systematic absences and confirmed by successful refinement of the structure. All possible alternatives *Pnma* (for compound **1**) and *Cc* (for **2** and **3**) were tried but did not give any reasonable solution. The structures were solved by a combination of direct methods (SIR 88)[18] and Fourier-difference techniques. The structures were refined by full-matrix least-squares analysis on *F* with anisotropic displacement parameters for all metal atoms. All hydrogen atoms of the organic moieties were generated in their idealized positions while hydride atom positions were estimated by potential-energy calculations.[19] All calculations were performed on a Silicon Graphics workstation using the TEXSAN software package.[20]

Atomic coordinates, thermal parameters and bond lengths and angles have been deposited at the Cambridge Crystallographic Data Centre (CCDC). See Instructions for Authors, *J. Chem. Soc., Dalton Trans.*, 1996, Issue 1. Any request to the CCDC for this material should quote the full literature citation and the reference number 186/127.

Results and Discussion

Syntheses

4-(*p*-Ferrocenylphenyl)pyridine **1** was prepared as described earlier by the one-step palladium(0)-catalysed aromatic cross-coupling reaction of organozinc with aryl bromide (Scheme 1).[12a] The complexes [$M_3(\mu\text{-}H)(CO)_{10}\{\mu\text{-}NC_5H_3C_6H_4(\eta^5\text{-}C_5H_4)Fe(\eta^5\text{-}C_5H_5)\}$] (M = Ru **2** or Os **3**) are oxidative-addition products of the reaction of [$Ru_3(CO)_{12}$] and [$Os_3(CO)_{10}(NCMe)_2$], respectively, with **1** (Scheme 1). The formation of both poses no conceptual problems. They are the results of orthometallation of the pyridyl ring in **1** accompanied by C–H bond cleavage α to the nitrogen-donor atom and loss of CO or MeCN ligands.[21] Subsequent chromatographic purification led to the isolation of **2** and **3** as stable orange solids in respectively 60 and 68% yields. Both cluster complexes dissolve readily in hydrocarbon solvents such as hexane. However, **2** undergoes slow decomposition at room temperature if it is allowed to stand in the solution state for a prolonged time.

The molecular formulae of compounds **2** and **3** were initially

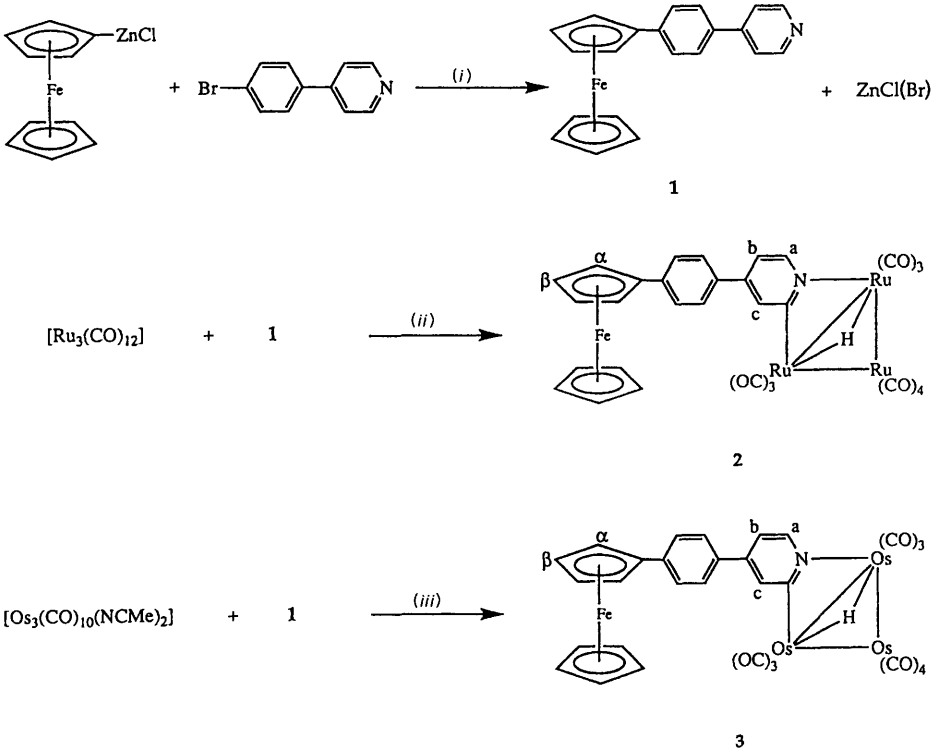

Scheme 1 (*i*) Pd^0; (*ii*) thf, heat; (*iii*) CH_2Cl_2, heat

established by elemental analyses and FAB mass spectrometry, and the spectroscopic properties are in accordance with their formulation. The complexes have many common spectral features. The IR carbonyl spectra are very similar in pattern to those of the μ-pyridyl clusters $[Os_3(\mu\text{-}H)(CO)_{10}(\mu\text{-}NC_5H_3R)]$ (R = H or alkyl)[21] and of other related orthometallated nitrogen-heterocyclic compounds.[22] This supports the N, C mode of attachment to the metal atoms. The ^1H NMR spectra of **2** and **3** in CD_2Cl_2 further confirm orthometallation of the heterocycle. The three pyridyl protons H_a–H_c are mutually coupled with each other to give three sets of double doublets with $J(H_aH_b)$, $J(H_bH_c)$ and $J(H_aH_c)$ = 6.1, 2.2 and 0.7 Hz, respectively. The most downfield signal is assigned to the hydrogen *ortho* to nitrogen which integrates as one proton against the hydride signal. The C_6H_4 moiety appears as a singlet for both complexes. The ferrocenyl ligands in **2** and **3** give rise to the usual patterns where the unsubstituted C_5H_5 ring displays a strong singlet at essentially the same position as that of **1** itself and the monosubstituted C_5H_4 ring gives an unsymmetrical pair of triplets corresponding to the spectrum of an A_2B_2 case with J(adjacent) ≈ J(cross). These triplets appear at the low-field side of the C_5H_5 singlet, indicating that all C_5H_4 protons are deshielded by the aryl ring bearing the ferrocene donor. The positions of these triplets for **1** and **3** are virtually the same but they are somewhat upfield shifted by *ca.* 0.08 ppm for **2**.

Conceptually, compounds **2** and **3**, the so-called supermolecules, are actually composed of molecular subunits that are capable of separate existence. The systems dealt with here are supermolecules of the type A–L–B, in which two active molecular components (A and B) are covalently linked *via* a suitable spacer (L).[23] The ferrocenyl and trinuclear carbonyl cluster moieties are the most important constituents of these molecules since they have distinct spectroscopic, photophysical and redox properties which determine to a large extent the behaviour of the supermolecules.

Electronic absorption spectra

Table 1 presents the electronic spectral data for the two new complexes in CH_2Cl_2 at room temperature. The spectra of ferrocene,[24] compound **1**[12a] and the orthometallated pyridyl analogues of **2** and **3** $[M_3(\mu\text{-}H)(CO)_{10}(\mu\text{-}NC_5H_4)]$ (M = Ru or Os)[25] are also included for comparison. The UV–VIS spectrum of **1** essentially consists of π ⟶ π* ligand transitions at 265 and 301 nm[26] and ferrocene charge-transfer bands at 357 and 456 nm.[27] The orange colour of **1** is in fact due to the ferrocene group [$\lambda_{max}(CH_2Cl_2)$ 456 nm, ε 860 $dm^3\ mol^{-1}\ cm^{-1}$]. Owing to its relatively small absorption coefficient, the ferrocenyl absorption in the visible region cannot easily be discerned in the spectra. The red shift of the ferrocenyl bands of **1** relative to those at 327 and 442 nm for ferrocene itself directly reflects the electron-withdrawing character of the 4-phenylpyridine substituent. The spectra of both **2** and **3** in CH_2Cl_2 exhibit intense bands in the UV range 238–318 nm due to ligand-based π ⟶ π* transitions. In the visible region an additional broad absorption band is observed around 421 nm for **2** whereas a band at 392 nm accompanied by a shoulder at 462 nm is present for the osmium counterpart. By comparing with the spectra of $[M_3(\mu\text{-}H)(CO)_{10}(\mu\text{-}NC_5H_4)]$ (M = Ru or Os) as well, we conclude that these are most likely a combination of absorption bands arising from both ferrocenyl and cluster fragments overlapping each other. Hence specific assignment is not possible.

Table 1 The UV/VIS spectral data for compounds **1–3** and related complexes[a]

Compound	λ_{max}/nm ($10^{-3}\varepsilon$/$dm^3\ mol^{-1}\ cm^{-1}$)
Ferrocene[b]	327 (0.05), 442 (0.09)
1	265 (12.7), 301 (14.8), 357 (2.72), 456 (0.86)
2	238 (36.09), 276 (29.56), 314 (31.20), 421 (9.92)
3	242 (37.69), 286 (33.71),[c] 318 (36.10), 392 (19.25), 462 (2.94)[c]
$[Ru_3H(CO)_{10}(\mu\text{-}NC_5H_4)]$	234 (24.23), 322 (7.18),[c] 422 (4.19)
$[Os_3H(CO)_{10}(\mu\text{-}NC_5H_4)]$	242 (26.53), 278 (18.48),[c] 332 (7.76), 386 (11.36)

[a] In CH_2Cl_2. [b] In MeCN. [c] Shoulder.

Electrochemistry

The electrochemical properties of the supramolecular cluster complexes **2** and **3** were investigated in CH_2Cl_2 using cyclic voltammetry with $[NBu_4]BF_4$ as the supporting electrolyte. Redox potential values obtained in this study are in Table 2. The ferrocenyl residue in **1** is characterized by a reversible (ΔE_p = 52 mV) wave at 0.22 V *vs.* Ag–$AgNO_3$ in CH_2Cl_2. When compared to ferrocene ($E_{\frac{1}{2}}$ = 0.17 V), this wave is anodically shifted by 50 mV. The shift is ascribed to conjugation of the ferrocenyl group to the electron-deficient pyridyl ring *via* the phenyl bridge, which makes removal of the electron from the ferrocene core more difficult. Such an increase in redox potential is also observed in 3- or 4-ferrocenylpyridine[28] and related molecules.[24,29] This indicates that there is good agreement between results from electrochemical and spectroscopic studies for **1**. The electrochemical response of **2** and **3** is a reversible one-electron oxidation centred on the ferrocenyl moiety and an irreversible oxidation at far greater potentials. Unexpectedly, it is quite evident from the $E_{\frac{1}{2}}$ values that the reversible ferrocenium–ferrocene couple of **2** and **3** is fairly insensitive to the electronic effect of the trinuclear cluster unit, excluding the existence of any substantial electronic interaction between them. Instead they undergo irreversible oxidations at 0.78 and 0.88 V respectively, close to the oxidation potentials for their pyridyl analogues $[M_3(\mu\text{-}H)(CO)_{10}(\mu\text{-}NC_5H_4)]$ (M = Ru, 0.80; M = Os, 0.92 V).[25] We can thus be sure that this irreversible oxidation is cluster based and variation of the substituent on the pyridyl ligand does not appear to affect the oxidation potential of the cluster fragment to a significant extent.

Molecular structures of compounds 1–3

An ORTEP[30] view of molecule **1** with the atom-numbering scheme, is shown in Fig. 1. Selected bond distances and angles are listed in Table 4. In the solid state molecule **1** consists of a ferrocene unit appended to the 4-phenylpyridine moiety in the *para* position. The two cyclopentadienyl rings of the ferrocene moiety are planar and almost parallel with a small ring tilt of 3.1°. They appear to be staggered to within 5°. The iron distances to the substituted and unsubstituted rings are 1.659

Table 2 Electrochemical data for complexes **1–3** and related molecules in CH_2Cl_2 at 298 K[a]

	Redox potential/V	
Compound	$E_{\frac{1}{2}}(\Delta E_p)$[b]	E_{ox}[c]
1	0.22 (52)	–
2	0.21 (78)	0.78
3	0.22 (74)	0.88
$[Ru_3H(CO)_{10}(\mu\text{-}NC_5H_4)]$	–	0.80
$[Os_3H(CO)_{10}(\mu\text{-}NC_5H_4)]$	–	0.92

[a] Analyses performed in dry, deoxygenated CH_2Cl_2 solutions containing 0.2 mol dm^{-3} $[NBu_4]BF_4$, scan rate 50 mV s^{-1}. [b] Half-wave potential values $E_{\frac{1}{2}}$ refer to the ferrocenium-ferrocene couple, $\Delta E_p = E_{pa} - E_{pc}$ mV, where E_{pa} and E_{pc} are respectively the anodic and cathodic peak potentials. [c] Values refer to the cluster-based oxidation process; all irreversible.

Table 3 Summary of crystal data, details of intensity collection and least-squares refinement parameters for compounds **1–3**

	1	**2**	**3**
Empirical formula	$C_{21}H_{17}FeN$	$C_{31}H_{17}FeNO_{10}Ru_3$	$C_{31}H_{17}FeNO_{10}Os_3$
M	339.22	922.53	1189.92
Crystal colour, habit	Orange, plate	Orange, plate	Orange, plate
Crystal size/mm	0.11 × 0.36 × 0.39	0.10 × 0.24 × 0.40	0.12 × 0.32 × 0.36
Crystal system	Orthorhombic	Monoclinic	Monoclinic
Space group	$Pna2_1$ (no. 33)	$C2/c$ (no. 15)	$C2/c$ (no. 15)
a/Å	27.494(4)	48.940(8)	48.997(7)
b/Å	9.630(3)	9.274(4)	9.239(4)
c/Å	5.841(3)	14.274(7)	14.243(6)
β/°		103.76(3)	103.85(3)
U/Å^3	1546.5(7)	6292(3)	6260(3)
Z	4	8	8
D_c/g cm^{-3}	1.457	1.947	2.525
$F(000)$	704	3584	4352
μ(Mo-Kα)/cm^{-1}	9.72	19.23	126.44
ω-Scan width/°	0.58 + 0.35 tan θ	0.58 + 0.35 tan θ	0.68 + 0.35 tan θ
2θ Range collected/°	2–50	2–45	2–45
Scan speed/° min^{-1}	16	16	16
Transmission coefficients	0.8878–1.0000	0.7814–1.0000	0.4240–1.0000
No. reflections collected	1631	4478	4457
No. unique reflections	1631	4419	4398
R_{int}	—	0.028	0.031
No. observed reflections [$I > 3\sigma(I)$]	1036	2940	2171
R^a	0.034	0.049	0.071
R'^b	0.027	0.047	0.062
g In weighting scheme	0.002	0.005	0.007
Goodness of fit	1.64	2.12	2.43
Maximum Δ/σ	0.08	0.07	0.05
No. parameters	208	205	205
Maximum, minimum density in ΔF map/e Å^{-3}	0.26, −0.22	0.94, −0.91	3.30, −3.00 (both close to Os)

^{a} $R = \Sigma||F_o| - |F_c||/\Sigma|F_o|$. ^{b} $R' = [\Sigma w(|F_o| - |F_c|)^2/\Sigma wF_o^2]^{\frac{1}{2}}$; $w = 4[\sigma^2(F_o^2) + gF_o^2]$.

and 1.663 Å, respectively. The mean Fe–C (C_5 rings) and C–C (C_5 rings) distances of 2.050 and 1.412 Å respectively are similar to those found in 4-biphenylferrocene[31] and other ferrocene derivatives.[32] All the aromatic bond lengths are within the expected ranges. The η^5-C_5H_4 fragment of the ferrocenyl group is not coplanar with the six-membered phenyl and pyridyl rings, the dihedral angles between them being respectively 10.7 and 8.8°. The pyridyl ring is rotated about C(14)–C(17) by 1.9° with respect to the phenyl plane to which it is covalently bonded.

The most striking feature of the structure is the non-centrosymmetric crystal packing of the molecules due to crystallization in the space group $Pna2_1$. The combined effect of the observed non-centric space group as well as its donor–π-acceptor structural motif renders a potential material for second-order non-linear optics.[33]

An ORTEP drawing of complexes **2** and **3** is shown in Fig. 2 along with the atom-numbering scheme. Pertinent structural parameters are given in Table 5. The essential features of both structures are very similar, so they will not be discussed separately. The structure of each complex reveals an ortho-metallation of the pyridyl ring, arising from C–H fission and transfer of an *o*-hydrogen atom to the metal. This is consistent with the structural assignment from spectroscopic studies and is directly related to the structure of the cluster [Os_3(μ-H)$(CO)_{10}$(μ-NC_5H_4)].[21a] However, to our knowledge, no ruthenium analogue of such a bridging 2-pyridyl complex has previously been reported. So complex **2** represents the first structurally characterized example of this class of ruthenium cluster complexes. Structurally, both compounds **2** and **3** can be regarded as possessing a trinuclear cluster unit [M_3(μ-H)$(CO)_{10}$(μ-NC_5H_4)] (M = Ru or Os) and a ferrocenyl donor covalently linked by a phenyl ring. The ferrocene-containing metallated pyridyl group is found to bridge one metal–metal edge [Ru(2)–Ru(3) in **2** and Os(2)–Os(3) in **3**] of the metal triangle to afford a four-membered ring containing M(2), M(3), C(11) and N (M = Ru **2** or Os **3**). The four-membered ring is at 103.0° to the Ru_3 plane in **2** and 102.9° to the Os_3 plane in **3**.

Table 4 Selected bond distances (Å) and angles (°) for Complex **1**

Fe–C(1)	2.047(6)	Fe–C(2)	2.049(7)
Fe–C(3)	2.038(7)	Fe–C(4)	2.044(6)
Fe–C(5)	2.041(6)	Fe–C(6)	2.066(6)
Fe–C(7)	2.064(6)	Fe–C(8)	2.050(7)
Fe–C(9)	2.042(6)	Fe–C(10)	2.057(5)
Fe–ring(C_5H_5)	1.663	Fe–ring(C_5H_4)	1.659
C(10)–C(11)	1.497(7)	C(14)–C(17)	1.505(7)
N–C(19)	1.332(8)	N–C(20)	1.332(9)
C(19)–N–C(20)	115.3(6)	C(13)–C(14)–C(17)	121.4(6)
C(15)–C(14)–C(17)	120.9(6)	C(6)–C(10)–C(11)	125.7(6)
C(9)–C(10)–C(11)	126.5(6)		

Dihedral angles between planes

A and B	1.9	A and C	8.8
B and C	10.7	C and D	3.1

Planes: A, defined by atoms N–C(19)–C(18)–C(17)–C(21)–C(20); B, C(11)–C(12)–C(13)–C(14)–C(15)–C(16); C, C(6)–C(7)–C(8)–C(9)–C(10); D, C(1)–C(2)–C(3)–C(4)–C(5).

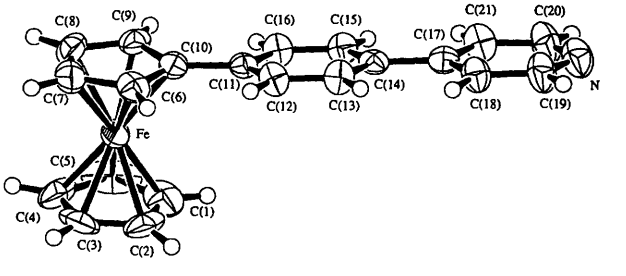

Fig. 1 An ORTEP drawing of complex **1** showing the atom-labelling scheme for non-hydrogen atoms. Thermal ellipsoids are drawn at the 50% probability level

The pyridyl ring is planar with a mean deviation from the plane of 0.004 Å for each complex. The dihedral angle between the pyridyl ring and the four-membered metallocycle which shares

Table 5 Selected bond distances (Å) and angles (°) for complexes **2** and **3**

	2 (M = Ru)	**3** (M = Os)			
M(1)–M(2)	2.854(1)	2.873(2)	M(1)–M(3)	2.870(1)	2.892(2)
M(2)–M(3)	2.900(1)	2.923(2)	M(2)–N	2.126(8)	2.13(2)
M(3)–C(11)	2.10(1)	2.13(3)	N–C(11)	1.34(1)	1.38(3)
N–C(15)	1.36(1)	1.36(3)	C(13)–C(16)	1.48(1)	1.45(4)
C(19)–C(22)	1.49(1)	1.55(5)	Fe–C(22)	2.04(1)	2.03(3)
Fe–C(23)	2.04(1)	2.02(4)	Fe–C(24)	2.03(1)	2.08(4)
Fe–C(25)	2.03(1)	2.03(4)	Fe–C(26)	2.03(1)	2.00(3)
Fe–C(27)	2.05(1)	2.04(4)	Fe–C(28)	2.05(1)	2.04(4)
Fe–C(29)	2.03(1)	2.04(4)	Fe–C(30)	2.04(1)	2.06(4)
Fe–C(31)	2.04(1)	2.07(4)	Fe–ring(C_5H_5)	1.658	1.656
Fe–ring(C_5H_4)	1.634	1.640			
M(2)–M(1)–M(3)	60.88(3)	60.95(5)	M(1)–M(2)–M(3)	59.83(3)	59.86(5)
M(1)–M(3)–M(2)	59.29(3)	59.23(5)	M(3)–M(2)–N	68.2(2)	68.1(6)
M(2)–M(3)–C(11)	68.4(3)	69.6(8)	M(2)–N–C(11)	110.8(6)	112(1)
M(3)–C(11)–N	112.6(7)	109(2)	C(11)–N–C(15)	121.8(8)	119(2)
C(13)–C(16)–C(17)	121(1)	126(3)	C(13)–C(16)–C(21)	122(1)	120(3)
C(19)–C(22)–C(23)	125(1)	126(3)	C(19)–C(22)–C(26)	126(1)	123(3)

Dihedral angles between planes

A and B	103.0	102.9	B and C	3.8	2.8
C and D	27.7	27.5	C and E	26.5	25.1
D and E	5.0	4.6	E and F	2.2	2.5

Planes: A, defined by atoms M(1)–M(2)–M(3); B, M(2)–M(3)–C(11)–N; C, N–C(11)–C(12)–C(13)–C(14)–C(15); D, C(16)–C(17)–C(18)–C(19)–C(20)–C(21); E, C(22)–C(23)–C(24)–C(25)–C(26); F, C(27)–C(28)–C(29)–C(30)–C(31)

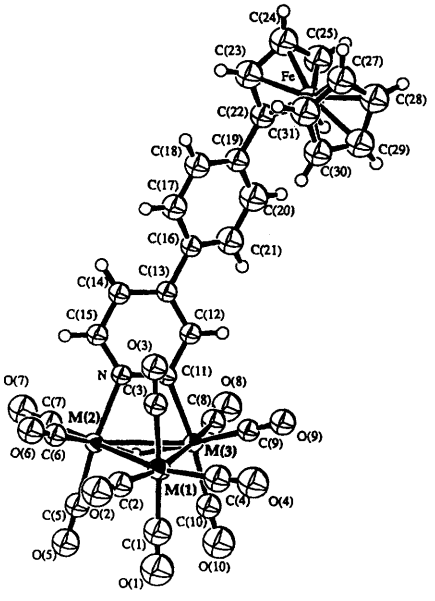

Fig. 2 An ORTEP drawing of complexes **2** (M = Ru) and **3** (M = Os) showing the atom-labelling scheme for non-hydrogen atoms. Thermal ellipsoids are drawn at the 50% probability level

a common edge N–C(11) is respectively 3.8 and 2.8° for **2** and **3**. Each also contains one bridging hydride, which was located using the potential-energy minimization procedure of Orpen,[19] and ten terminal carbonyl ligands. The hydride ligand also bridges the edge Ru(2)–Ru(3) for **2** and Os(2)–Os(3) for **3**. In terms of electron counting, each cluster is electron precise with 48 cluster valence electrons if the 2-pyridyl bridging ligand is considered as a three-electron donor. The dibridged metal–metal bond is the longest of the three [Ru(2)–Ru(3) 2.900(1) in **2** and Os(2)–Os(3) 2.923(2) Å in **3**]. The other two non-bridged metal–metal bonds in each structure are normal at 2.854(1) and 2.870(1) Å for **2** and 2.873(2) and 2.892(2) Å for **3**.

As far as the conformation of the cyclopentadienyl rings of the ferrocenyl group in each complex is concerned, the eclipsed nature of the rings is confirmed by the X-ray structural determination and contrasts with the staggered conformation observed in $[Os_3(\mu\text{-}H)_2(CO)_9\{\mu_3\text{-}CNC_5H_4C_6H_4(\eta^5\text{-}C_5H_4)\text{-}Fe(\eta^5\text{-}C_5H_5)\}]$[12a] recently reported. It has previously been pointed out that the energy difference between the two conformers is rather small and the stability order may be altered easily through introduction or variation of substituents on the cyclopentadienyl rings.[33] In both cases the five-membered rings do not deviate significantly from planarity and they are nearly parallel, with very small ring tilt angles (2.2° for **2** and 2.5° for **3**) and produce an average distance of 1.646 (**2**) or 1.648 Å (**3**) from their centroids to the iron atom. The substituted η^5-C_5H_4 ring is not coplanar with the phenyl and pyridyl planes. In addition, these two six-membered aromatic moieties are twisted with respect to each other and the dihedral angle between them is 27.7° for **2** and 27.5° for **3**. The average C–C bond length in both cyclopentadienyl rings is 1.412 and 1.416 Å, respectively for **2** and **3**, whereas the corresponding mean Fe–C (cyclopentadienyl) distance is 2.038 and 2.041 Å. The remaining interatomic distances and angles in the molecules are normal and compare well with the values reported for other ferrocene and cluster derivatives.[12a,35]

Conclusion

A new class of metallosupramolecular cluster complexes bearing a trinuclear carbonyl cluster unit covalently appended to a redox-active ferrocenyl centre by a phenyl bridge has been prepared and structurally characterized by X-ray crystallography. These new cluster complexes are electrochemically active and cyclic voltammetric studies on CH_2Cl_2 solutions reveal that they undergo a reversible one-electron oxidation centred on ferrocene the $E_{\frac{1}{2}}$ value of which is not influenced by the electronic effect of the cluster core. An irreversible oxidation associated with the cluster unit is observed at more anodic potential.

Acknowledgements

We gratefully acknowledge financial support from the Hong Kong Research Grants Council and the University of Hong

Kong. W.-Y. W. thanks the Croucher Foundation for financial support.

References

1 E. C. Constable, R. Martinez-Máñez, A. M. W. Cargill Thompson and J. V. Walker, *J. Chem. Soc., Dalton Trans.*, 1994, 1585; D. Astruc, *New J. Chem.*, 1992, **16**, 305; J. P. Sauvage, J. P. Collin, J. C. Chambron, S. Guillerez, C. Coudret, V. Balzani, F. Barigelletti, L. De Cola and L. Flamigni, *Chem. Rev.*, 1994, **94**, 993.

2 C. Kollmar, M. Couty and O. Kahn, *J. Am. Chem. Soc.*, 1991, **113**, 7994; J. S. Miller, A. J. Epstein and W. M. Reiff, *Chem. Rev.*, 1988, **88**, 201; J. S. Miller and A. J. Epstein, *Angew. Chem., Int. Ed. Engl.*, 1994, **33**, 385.

3 R. W. Wagner, P. A. Brown, T. E. Johnson and J. S. Lindsey, *J. Chem. Soc., Chem. Commun.*, 1991, 1463; E. C. Constable, *Angew. Chem., Int. Ed. Engl.*, 1991, **30**, 407; P. D. Beer, Z. Chen, M. G. B. Drew and A. J. Pilgrim, *Inorg. Chim. Acta*, 1994, **225**, 137.

4 B. Delavaux-Nicot, R. Mathieu, D. De Montauzon, G. Lavigne and J. P. Majoral, *Inorg. Chem.*, 1994, **33**, 434; I. R. Butler, *Organometallic Chemistry*, ed. E. W. Abel, Specialist Periodic Reports 21, Royal Society of Chemistry, Cambridge, 1992, p. 338.

5 A. Werner and W. Friedrichsen, *J. Chem. Soc., Chem. Commun.* 1994, 365; R. Deschenaux, I. Kosztics, U. Scholten, D. Guillon and M. Ibn-Elhaj, *J. Mater. Chem.*, 1994, **4**, 1351.

6 M. C. B. Colbert, A. J. Edwards, J. Lewis, N. J. Long, N. A. Page, D. G. Parker and P. R. Raithby, *J. Chem. Soc., Dalton Trans.*, 1994, 2589; K. L. Kott, D. A. Higgins, R. J. McMahon and R. L. Corn, *J. Am. Chem. Soc.*, 1993, **115**, 5342; S. Ghosal, M. Samoc, P. N. Prasad and J. J. Tufariello, *J. Phys. Chem.*, 1990, **94**, 2847; Z. Yuan, N. J. Taylor, Y. Sun, T. B. Marder, I. D. Williams and L. T. Cheng, *J. Organomet. Chem.*, 1993, **449**, 27; Z. Yuan, G. Stringer, T. R. Jobe, D. Kreller, K. Scott, L. Koch, N. J. Taylor and T. B. Marder, *J. Organomet. Chem.*, 1993, **452**, 115.

7 L. T. Phang, S. C. F. Au-Yeung, T. S. A. Hor, S. B. Khoo, Z. Y. Zhou and T. C. W. Mak, *J. Chem. Soc., Dalton Trans.*, 1993, 165; M. Sato, H. Shintate, K. Kawata, M. Sekino, M. Katada and S. Kawata, *Organometallics*, 1994, **13**, 1956.

8 R. Bosque, M. Font-Bardia, C. Lopez, J. Sales, J. Silver and X. Solans, *J. Chem. Soc., Dalton Trans.*, 1994, 747; A. Togni, M. Hobi, G. Rihs, G. Rist, A. Albinati, P. Zanello, D. Zech and H. Keller, *Organometallics*, 1994, **13**, 1224; S. B. Wilkes, I. R. Butler, A. E. Underhill, A. Kobayashi and H. Kobayashi, *J. Chem. Soc., Chem. Commun.*, 1994, 53.

9 N. Rösch, L. Ackermann, G. Pacchioni and B. I. Dunlap, *J. Chem. Phys.*, 1991, **95**, 7005; I. H. Williams, D. Spangler, D. A. Femec, G. M. Maggiora and R. L. Schowen, *J. Am. Chem. Soc.*, 1980, **102**, 6621; D. C. Johnson, P. P. Edwards, R. E. Benfield, W. J. H. Nelson and M. D. Vargas, *Nature (London)*, 1985, **314**, 231; A. J. Blake, A. Harrison, B. F. G. Johnson, E. J. L. McInnes, S. Parsons, D. S. Shephard and L. J. Yellowlees, *Organometallics*, 1995, **14**, 3160; L. F. Dahl, W. L. Olsen and A. M. Stacy, *J. Am. Chem. Soc.*, 1986, **108**, 7646.

10 J. J. Schneider, R. Goddard, C. Kröger, S. Werner and B. Metz, *Chem. Ber.*, 1991, **124**, 301.

11 E. C. Constable, A. J. Edwards, R. Martinez-Máñez, P. R. Raithby and A. M. W. Cargill Thompson, *J. Chem. Soc., Dalton Trans.*, 1994, 645; C. Chambron, C. Coudret and J. P. Sauvage, *New J. Chem.*, 1992, **16**, 361; P. D. Beer, *Chem. Soc. Rev.*, 1989, **18**, 409; C. D. Hall, J. H. R. Tucker and N. W. Sharpe, *Organometallics*, 1991, **10**, 1727; J. C. Medina, I. Gay, Z. Chen, L. Echengoyen and G. W. Gokel, *J. Am. Chem. Soc.*, 1991, **113**, 365.

12 (*a*) W. Y. Wong, W. T. Wong and K. K. Cheung, *J. Chem. Soc., Dalton Trans.*, 1995, 1379; (*b*) G. H. Worth, B. H. Robinson and J. Simpson, *Organometallics*, 1992, **11**, 501; (*c*) J. Borgdorff, E. J. Ditzel, N. W. Duffy, B. H. Robinson and J. Simpson, *J. Organomet. Chem.*, 1992, **437**, 323.

13 N. G. Connelly and W. E. Geiger, *Adv. Organomet. Chem.*, 1984, **23**, 1.

14 D. D. Perrin, W. L. F. Armarego and D. R. Perrin, *Purification of Laboratory Chemicals*, 2nd edn., Pergamon, Oxford, 1980.

15 J. N. Nicholls and M. D. Vargas, *Inorg. Synth.*, 1990, **28**, 289.

16 A. C. T. North, D. C. Phillips and F. S. Mathews, *Acta Crystallogr., Sect. A*, 1968, **24**, 351.

17 D. T. Cromer and J. T. Waber, *International Tables for X-Ray Crystallography*, Kynoch Press, Birmingham, 1974, vol. 4, (*a*) Table 2.2B; (*b*) Table 2.3.1.

18 M. C. Burla, M. Camalli, G. Cascarano, C. Giacovazzo, G. Polidori, R. Spagna and D. Viterbo, *J. Appl. Crystallogr.*, 1989, **22**, 389.

19 A. G. Orpen, *J. Chem. Soc., Dalton Trans.*, 1980, 2509.

20 TEXSAN, Crystal Structure Analysis Package, Molecular Structure Corporation, Houston, TX, 1985 and 1992.

21 (*a*) C. C. Yin and A. J. Deeming, *J. Chem. Soc., Dalton Trans.*, 1975, 2091; (*b*) A. J. Deeming, R. Peters, M. B. Hursthouse and J. D. J. Backer-Dirks, *J. Chem. Soc., Dalton Trans.*, 1982, 787.

22 A. J. Arce, C. Acuña and A. J. Deeming, *J. Organomet. Chem.*, 1988, **356**, C47.

23 V. Balzani and F. Scandola, *Supramolecular Photochemistry*, Ellis Horwood, Chichester, 1991, chs. 3 and 5.

24 J. C. Chambron, C. Coudret and J. P. Sauvage, *New J. Chem.*, 1992, **16**, 361.

25 W. Y. Wong and W. T. Wong, unpublished work.

26 M. L. Stone and G. A. Crosby, *Chem. Phys. Lett.*, 1981, **79**, 169.

27 Y. S. Sohn, D. N. Hendrickson and H. B. Gray, *J. Am. Chem. Soc.*, 1971, **93**, 3603.

28 T. M. Miller, J. A. Kazi and M. S. Wrighton, *Inorg. Chem.*, 1989, **28**, 2347; O. Carugo, G. De Santis, L. Fabbrizzi, M. Licchelli, A. Monichino and P. Pallavicini, *Inorg. Chem.*, 1992, **31**, 765.

29 B. Farlow, T. A. Nile, J. L. Walsh and A. T. McPhail, *Polyhedron*, 1993, **12**, 2891.

30 C. K. Johnson, ORTEP, Report ORNL-5138, Oak Ridge National Laboratory, Oak Ridge, TN, 1976.

31 F. H. Allen, J. Trotter and C. S. Williston, *J. Chem. Soc. A*, 1970, 907.

32 C. Lopez, J. Sales, X. Solans and R. Zquiak, *J. Chem. Soc., Dalton Trans.*, 1992, 2321.

33 N. J. Long, *Angew. Chem., Int. Ed. Engl.*, 1995, **34**, 21 and refs. therein.

34 F. A. Cotton and G. Wilkinson, *Advanced Inorganic Chemistry*, 5th edn., Wiley, New York, 1988, p. 79.

35 A. J. Arce, P. A. Bates, S. P. Best, R. J. H. Clark, A. J. Deeming, M. B. Hursthouse, R. C. S. McQueen and N. I. Powell, *J. Chem. Soc., Chem. Commun.*, 1988, 478.

Received 8*th February* 1996; *Paper* 6/00949B